# Data analysis of a magnetotelluric transect across the SW Amazon craton

Clarisse Monteiro Fernandes (ON-COGE)*; Leonardo Guimarães Miquelutti (ON-COGE); Ved Prakash Maurya (ON-COGE); Emanuele Francesco La Terra (ON-COGE); Sergio Luiz Fontes (ON-COGE).



## Abstract

Broadband and long-period magnetotelluric data were collected along a 200 km long NNE-SSW transect at the southwest border of the Amazon Craton, in a volcanic to plutonic region related to the Alta Floresta/Juruena-Teles Pires Golden Province. The data were processed using a robust regression scheme over the EM cross-spectra for combined single and remote reference stations, producing estimated transference functions of good to intermediate quality. Those were submitted to geometric analysis to assess dimensionality and geoelectric preferred strikes by means of WAL invariants and phase tensor decomposition. Additionally phase tensor pseudosections were estimated, and compared with traditional apparent resistivity and phase in TE and TM modes plus tipper magnitude pseudosections. The obtained results suggest 3-D type regional structures moderately to highly distorted by 3-D local, smaller conductive bodies. A highly resistive block is shown in the central to the northern transect sector, for periods from $10^{-4}$ to $10^{0}$ seconds, including a resistant root at $10^{4}$ seconds in the central sector. Two main conductive anomalies are showed for periods from $10^{-4}$ to $10^{4}$: at the southern transect sector, which may be related to the sedimentary and felsic to intermediate volcanic units at the craton south border; and at the middle transect sector, which may be related to intermediate to basaltic volcanic units that overlay the contact between the craton and the Precambrian sedimentary cover.

## Introduction

The magnetotelluric method is largely employed on regional to global, deep-probing geophysical studies and, in the last decades, on mineral industry exploration studies. Past successful experiences have been reported in magnetotelluric soundings over very resistive lithospheric regions containing large scale conductive anomalies as, for example, cratonic regions embodying metalliferous deposits (Heinson *et al.*, 2006; Maier *et al*., 2007; Spratt *et al.,* 2014). A question that arises is how to deal with distortion of magnetotelluric responses in such an extreme contrasting environment between usual high resistive bedrock and conductive ore bodies.

This work presents a first attempt to investigate the geoelectrical structural information depicted from a magnetotelluric transect across the Rondônia-Juruena and Tapajós-Parima tectonic provinces, south-west sector of the Amazonian Craton. This region comprises the Alta Floresta/Juruena-Teles Pires Golden Province, related to an ancient arc-accretion setting (Scandolara *et al*., 2017, Tassinari & Macambira, 2004). The specific aim of this study is the assessment of the geoelectric strikes, distortions, predominant structures and dimensionalities of the lithosphere. Several EM attributes are evaluated including WAL invariants derived from the magnetotelluric transfer functions, as well as the tipper transfer function relating the vertical magnetic field variations with the horizontal magnetic fields variations, and the phase tensor.

## Tectonic Setting

The Amazon Craton, one of the main tectonic units in the South American Platform, represents a stable lithospheric plate composed of Archean to Mesoproterozoic amalgamated provinces. The published proposed geotectonic models for this region can be grouped into two main competing approaches: the crustal reworking based (Amaral, 1974; Almeida, 1978; Issler, 1977; Hasui *et al*., 1984; e Costa & Hasui, 1997; *apud* Tassinari & Macambira, 2004) and the accretionary based (Cordani *et al*., 1979; Cordani & Brito Neves, 1982; Tassinari & Macambira, 1999; Tassinari *et al*., 2000; Santos *et al*., 2000; *apud* Tassinari & Macambira, 2004) tectonic models.

The crustal reworking based considers just structural analysis performed over aerogeophysical data, and foresees an Archean to Paleoproterozoic Craton composed by a group of twelve granite-greenstone paleo-plates, with granulite-composed collisional or shear belts which were constantly reactivated. The accretionary based model (Fig.1), otherwise proposed on geochronological ground and complementary petrological and restricted geologic mapping evidence, remains the most accepted among the geoscientists and represents the state-of-art of published, peer-reviewed models in terms of tectonics.

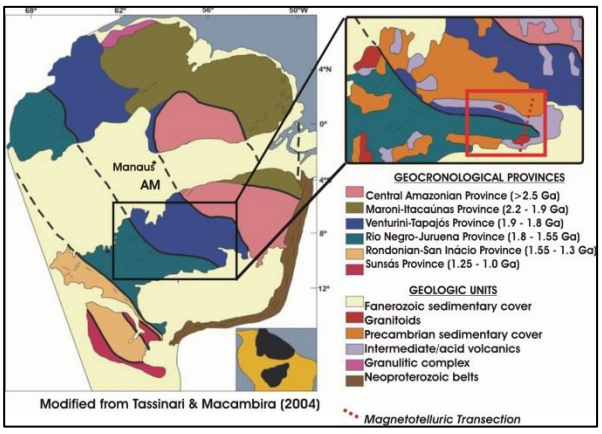


***Figure 1:*** *Accretionary model geologic map.*

This model describes a succession of juvenile melts episodes producing magmatic arcs which amalgamate the older, Archean crustal fragments, followed by a terminal stage of ensialic reworking, anorogenic magmatism and isotopic rejuvenation at the extreme southwest. Different types of geochronological methods of low- and high-resolution, produces slightly diverging sub-models, culminating in differences related to provinces boundaries and rock ages.

Besides that, new regional geologic maps and data continue being published, mainly by the Brazilian Geologic Service (CPRM), allowing refinements of the main models along with more radical reformulation (Scandolara *et al*., 2017), but that have not yet culminated in a refereed and broadly accepted geotectonic general model for the entire Craton.

**Method**

The magnetotelluric method uses the natural electromagnetic field variations recorded at the surface in order to probe the electrical conductivity distribution at depth associated with the Earth's subsurface structure. The natural electromagnetic signal source for the method are the MHD waves and pulsations produced by the solar plasma interaction with the terrestrial magnetosphere and ionosphere, for the low frequency or long period signal (0.0001 Hz or 10000 s), and the called “spherics” produced in the global atmospheric electrical circuit, for the high frequency or short period signal (10000Hz or 0.0001 s). The resulting electromagnetic field is delimited by an atmospheric waveguide that extends from the top of ionosphere to the Earth’s surface.

The magnetotelluric physical mathematics lays on two valid simplifications when considering a distance source and a period signal range restricted from 10000 to 0.0001 seconds: 1) the electromagnetic waves propagates in a vertical axis as plane waves from the atmospheric waveguide into the solid Earth, inducing secondary telluric currents in the subsurface and an associated magnetotelluric field; 2) a quasi-static approximation allows describing the propagating process in the atmospheric waveguide and in the solid Earth as diffusive by neglecting the Maxwell's displacement current correction.

The electromagnetic signal is acquired at the surface as temporal series and is composed by both the magnetotelluric fields and the external influences. The orthogonal components of the horizontal electric and magnetic fields are related via the most basic magnetotelluric transfer function, defining the complex *impedance tensor* $\bar{\bar{Z}}$:

$$\bar{E} = \bar{\bar{Z}}\,\bar{B}/\mu_0$$

The diagonal elements of the impedance tensor, $Z_{xx}$ and $Z_{yy}$, couple parallel electric and magnetic field components, while the off-diagonal components, $Z_{xy}$ and $Z_{yx}$, couple orthogonal electric and magnetic field components. Each component $Z_{ij}$ of $\bar{\bar{Z}}$ has associated apparent resistivity ($\rho_{a,ij}$) and phase ($\phi_{ij}$):

$$\rho_{a,ij} = \frac{1}{\mu 0 \omega}|Z_{ij}|^2 \text{ and } \phi_{ij} = tan^{-1}\left(\frac{Im\{Z_{ij}\}}{Re\{Z_{ij}\}}\right)$$

As a tensor, $\bar{\bar{Z}}$ contains information about dimensionality and electromagnetic geometry. The simple, regional undistorted regional geoelectric structure should be easily obtained by observing the components of the $\bar{\bar{Z}}$ tensor. In a unidimensional Earth the diagonal components of the impedance tensor are zero, whilst the off-diagonal components are equal in magnitude, but have opposite signs; in a bi-dimensional Earth, the diagonal components are equal in magnitude, but have opposite sign, whilst the off-diagonal components differ; in a tri-dimensional Earth, all components differ.

When real data sense local anisotropic structures, this simple decomposition fails, and the distortion must be assessed first. The *impedance tensor* $\bar{\bar{Z}}$ can be decomposed into regional and local sets of information, being local anisotropies regarded as galvanic distortion over the regional geoelectric structure, affecting only the measured electric field $\bar{E}^m$, so the regional electric field $\bar{E}^r$ is affected by a distortion matrix $\bar{\bar{D}}$ as $\bar{E}^m = \bar{\bar{D}}\,\bar{E}^r$. The regional transfer function expression is given by $\bar{E}^r = \bar{\bar{Z}}^r\,\bar{B}/\mu_0$, with $\bar{\bar{Z}}^r$being the regional impedance tensor, and the measured transfer function is $\bar{E}^m = \bar{\bar{Z}}^m\,\bar{B}/\mu_0$, and $\bar{\bar{Z}}^m$ being the measured impedance tensor. Comparing theses equations, we obtain:

$$\bar{\bar{D}}\,\bar{\bar{Z}}^r\bar{B}/\mu 0 = \bar{\bar{D}}\,\bar{E}^r = \bar{E}^m$$

So the impedance tensor, considering distortion is simply given by:

$$\bar{\bar{Z}}^m = \bar{\bar{D}}\,\bar{\bar{Z}}^r$$

A great number of techniques are employed to overcome the problems that arise for the critical distortion sceneries with varying geometries combinations for regional and local information. A type of approach summarized in Weaver *et al.* (2006) is recovering regional geometry considering the decomposition of tensors themselves derived from the traditional impedance tensor ($\bar{\bar{Z}}$): its equivalent *magnetotelluric tensor* ($\bar{\bar{M}}$), a variation of $\bar{\bar{Z}}$ computing $\bar{B}$ instead of $\bar{B}/\mu_0$ (=$\bar{H}$), given by $\bar{E} = \bar{\bar{M}}\,\bar{B}$; and the *phase tensor* ($\bar{\bar{\Phi}}$), a tensor that contain the phase information in $\bar{\bar{Z}}$. Together with those tensors, the *tipper vectors* ($\bar{T}$) can also assess the presence of conductivity anomalies. These approaches use the premise that the components concerning the magnetic field are unaffected by the distortion matrix $\bar{\bar{D}}$, considered just related to galvanic distortion.

The complex *tipper vector* ($\bar{T}$) represents the relationship between vertical and horizontal magnetic field components and can be decomposed into two induction vectors in the *xy* plane, corresponding to its real and imaginary parts, representing a projection of the vertical magnetic field onto the horizontal *xy* plane. The magnetic field in terms of components and tipper can be written as:

$$B_z = (T_x, T_y)\begin{pmatrix} B_x \\ B_y \end{pmatrix}$$

And so, tipper is decomposed into real and imaginary parts as:

$$\bar{T}^{re} = (Re(T_x), Re(T_y)) \text{ and } \bar{T}^{im} = (Im(T_x), Im(T_y))$$

That can be simple stated as *induction arrows*, showing the horizontal direction connected to the maximal vertical magnetic field and used to infer the presence of lateral variations in conductivity: their magnitude representing the induction magnitude and direction of its real part, in Parkinson convention, pointing towards the inductor, being simple $\bar{T}^{arrow} = (T_x, T_y)$.

The real *phase tensor* $\bar{\bar{\Phi}}$ , a tensor that contain the phase information in $\bar{\bar{Z}}$, theoretically is unaffected by galvanic distortion, and can be characterized by its rotational invariants, the semi-major tensor axis ($\Phi_{max}$), the semi-minor tensor axis ($\Phi_{min}$) and the parameter ß (skew angle), besides the additional parameters λ (ellipticity) and α (angle between the x-axis of the on the coordinate system and the principal tensor axis), with the orientation of the major axis given by α−ß. Considering a rotation matrix given by $\bar{\bar{R}}(\alpha + \beta)$, the phase tensor $\bar{\bar{\Phi}}$ is $\begin{pmatrix} \Phi_{xx} & \Phi_{xy} \\ \Phi_{yx} & \Phi_{yy} \end{pmatrix} = \bar{\bar{R}}^T(\alpha - \beta) \begin{pmatrix} \Phi_{max} & 0 \\ 0 & \Phi_{min} \end{pmatrix} \bar{\bar{R}}(\alpha + \beta)$, and then α, ß and λ are:

$$\alpha = \frac{1}{2} tan^{-1}\left(\frac{\Phi_{xy} + \Phi_{yx}}{\Phi_{xx} - \Phi_{yy}}\right), \quad ß = \frac{1}{2} tan^{-1}\left(\frac{\Phi_{xy} - \Phi_{yx}}{\Phi_{xx} + \Phi_{yy}}\right) \text{ and}$$

$$\lambda = \left(\frac{\Phi_{max} - \Phi_{min}}{\Phi_{max} + \Phi_{min}}\right)$$

The orientation of the major axis (α−ß) represents the phase tensor strike, an equivalent of the 2-D geoelectric strike and a preferential strike direction for 3-D structures. A combined analysis of ß and λ allow inferences about the dimensional nature of he studied region, suggesting an 1-D structure if both parameters are zero, and 3-D structure if they both are either non-zero or above some chosen threshold.

The complex *magnetotelluric tensor* $\bar{\bar{M}}$ can be decomposed into eight rotational invariants, from which dimensionality and distortion can be obtained. Decomposing $\bar{\bar{M}}$ in real and imaginary parts, we get:

$$\bar{\bar{M}} = \begin{pmatrix} \xi_1 + \xi_3 & \xi_2 + \xi_4 \\ \xi_2 - \xi_4 & \xi_1 - \xi_3 \end{pmatrix} + i \begin{pmatrix} \eta_1 + \eta_3 & \eta_2 + \eta_4 \\ \eta_2 - \eta_4 & \eta_1 - \eta_3 \end{pmatrix},$$

where $\xi_i$ and $\eta_i$can be related by $d_{ij}$:

$$d_{ij} = \frac{\xi_i \eta_j - \xi_j \eta_i}{(\xi_4^2 + \xi_1^2)^{1/2}(\eta_4^2 + \eta_1^2)^{1/2}}$$

And then the invariants are:

$$I_1 = (\xi_4^2 + \xi_1^2)^{1/2} \qquad I_2 = (\eta_4^2 + \eta_1^2)^{1/2}$$

$$I_3 = \frac{(\xi_2^2 + \xi_3^2)^{1/2}}{I_1} \qquad I_4 = \frac{(\eta_2^2 + \eta_3^2)^{1/2}}{I_1}$$

$$I_5 = \frac{\xi_4\eta_1 + \xi_1\eta_4}{I_1 I_2} \qquad I_6 = \frac{\xi_4\eta_1 - \xi_1\eta_4}{I_1 I_2}$$

$$I_7 = \frac{d_{41} - d_{23}}{Q}$$

$$Q = [((d_{12} - d_{34})^2 + (d_{13+}d_{24})^2)]^{1/2}$$

Their combined evaluation at established threshold values is used for dimensional analysis purposes.

The original transect consists of a 200 km profile comprising 35 magnetotelluric broadband stations 6 km spaced apart and complemented by 12 long period MT stations 18 km spaced (Fig.2), covering a wide range of periods ($10^{-4}$ to $10^4$ seconds), thus allowing to probe a wide depth range into the Earth. From those original 35 stations, 7 of them are considered of poor quality and will not be considered for analysis at this point.

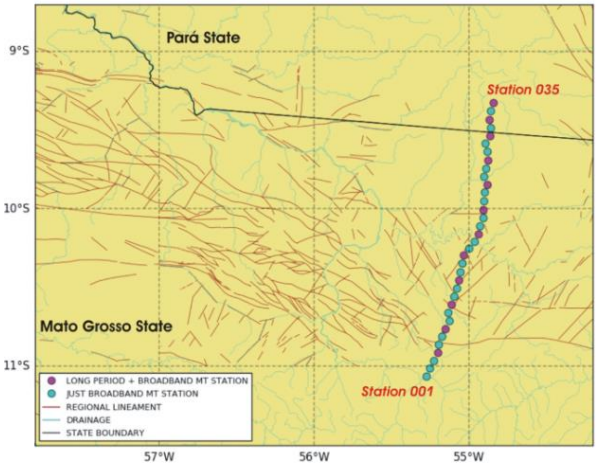


***Figure 2:*** *Map with MT stations for the studied transect*.

The processing scheme combine spectral analysis and robust regression, using the computational codes for single station and remote reference arrays contained in *EMTF* (Egbert & Booker; Egbert & Eisel, 1998). The spectral analysis considered adaptive, autoregressive pre-whitening filtering, followed by time series conversion to frequency domain by a combination of standard FFT and cascade decimation. The estimation of transference functions is done by robust regression M-estimate using coherence weighting criteria with established threshold of 0.8 (Egbert & Livelybrooks, 1996). It is worth to mention that the transect is in the zone around the magnetic dip equator, where significant source deviations are due to the presence of the equatorial electrojet; the segments affected by signal in disagreement with the plane wave assumption must be statistically down-weighted (Padilha, 1999; Padilha *et al*., 1997), justifying the coherence weighting procedure adopted for this study.

The obtained results are of good quality containing some pitfalls in a considerable number of stations. Galvanic distortion was expected due to the previous knowledge established about the geological setting and it is believed to be the cause of poor data quality at some stations. Considering such a scenario, besides discarding some stations, the geometric data analysis considered phase tensor decomposition and magnetotelluric tensor invariants' analysis to evaluate dimensionality, distortion and geoelectric strikes. Pseudo-sections based on phase tensor and magnetotelluric invariants parameters were produced and compared with traditional apparent resistivity and phase responses pseudosections. The computational codes used here were *WALDIM* from Martí *et al*. (2009), for invariants dimensional analysis based on Weaver *et al*. (2000) and Martí *et al.* (2005); the

*analysis* module of *MTpy toolbox* (Krieger & Peacock, 2014) for phase tensor and strike analysis as stated in Caldwell *et al.* (2004) and Bibby *et al.* (2005); and the use of the *WinGlink* software for conventional apparent resistivity, phase and tipper magnitude pseudosections.

## Results and Discussion

The dimensional analysis by phase tensor parameters (Fig.3) ellipticity and skew angle considered established threshold for 3-D as 0.2 for ellipticity, and ±4° for skew angle. The majority of data lay above thresholds, suggesting evident 3-D dimensionality.

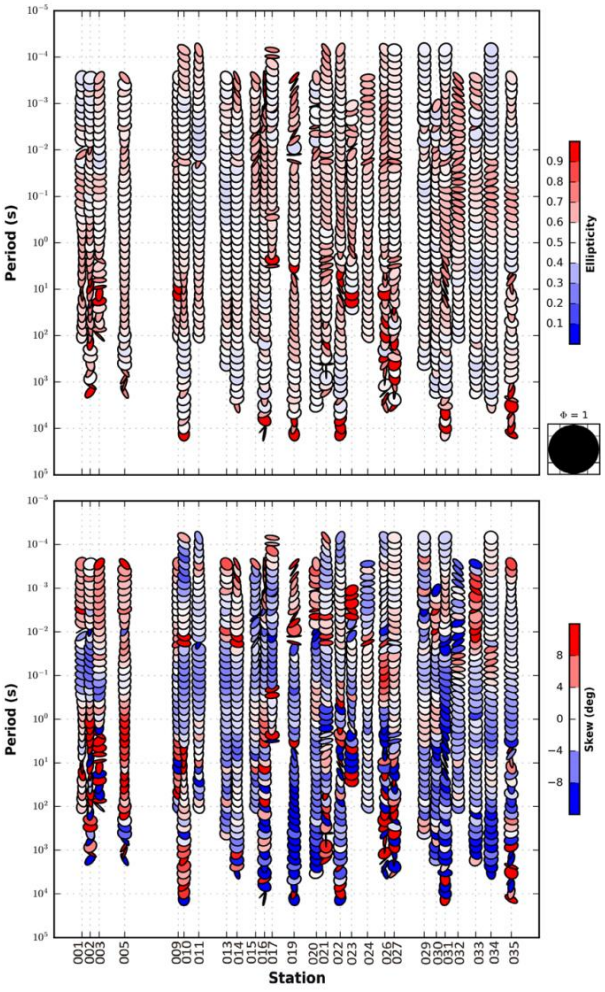


***Figure 3:*** *Dimensional analysis results by phase tensor parameters, ideally unaffected by distortion. The ellipse pseudosections, coloured by ellipticity and skew angle suggest a regional 3-D structure.*

The dimensional analysis by WAL invariants (Fig.4) considered 8 decade-period bands from $10^{-4}$ to $10^{4}$ seconds, and thresholds for invariants as 1.5 for I3 to I7, and 1.0 for Q, totalizing 1246 period slices to be analysed, from which 48% were considered purely 3-D and 26% were 2-D (or even 1-D) with some type of 3-D distortion. Just 9% of period slices were 1-D or 2-D without distortion, while 17% were considered undetermined.

These results suggest 3-D regional and anomalous local dimensionality, but also with the perspective of reasonable results with 2-D inversion restricted to an efficient distortion assessing and removal.

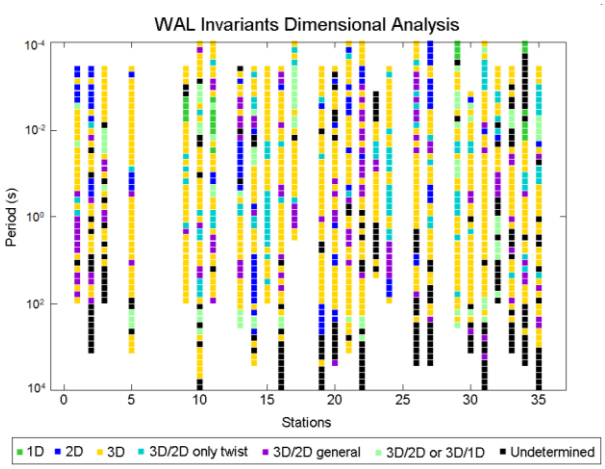


***Figure 4:*** *Dimensional and distortion analysis results by WAL invariants. The regional structure is 3-D, with localized 2-D distorted by 3-D anomalies.*

The strike analysis results (Fig.5) indicates the preferred directions considering a regional 3-D structure. We analysed the strike estimated from the invariants of the impedance tensor (Weaver et al., 2006), the phase tensor azimuth (Caldwell et al., 2004) and the strike obtained by tipper, considered orthogonal to the induction arrow direction. Geographic north is assumed, and magnetic declination is 18.35°W. The Z-invariants' strike analysis resulted in 137.5$^{o}$ for median and 150.0$^{o}$ for both mode and mean, while the phase tensor strike analysis yielded 141.8$^{o}$ for median, 150.0$^{o}$ for mode and 125.6$^{o}$ for mean. Complementing those regional strikes, the tipper strike were also computed, and resulted in 89.9$^{o}$ as median, and 150.0 $^{o}$ for both mode and mean.

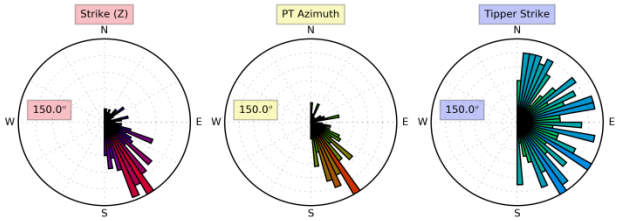


***Figure 5:*** *Preferential strikes estimated by Z-invariants, phase tensor azimuth, and tipper strike. Geoelectric regional strike can be approximated to NW-SE (330-150° azimuth); random tipper strikes must indicate small conductive bodies.*

Considering the geologic framework, the Z-invariants and phase tensor strikes are consistently NW-SE, displaying full consistence with the regional geology, being the Z-invariants' strike more scattered. The tipper estimates vary widely, possibly reflecting the fact that the most conductive structures do not have a preferential orientation, being 3-D in nature, as pointed by WAL invariants dimensional analysis.

Pseudo sections were obtained for the TE and TM modes of apparent resistivity and phase versus period, as well as for the tipper magnitude versus period, this scaled from 0 to 1.0 (Fig.6).

The presence of a highly resistive block in the central profile sector, embedded in a more conductive material can be observed in both TE and TM modes, but extends further north in the TM mode. The southernmost portion of transect is highly conductive for both TE and TM modes. The long period data observed in the TM mode bellow the resistive block is composed mainly by an almost continuous thick layer of highly conductive material, which is not depicted in the apparent resistivity section of the TE mode, but is clearly indicated in the phase values.

The phases in TE and TM modes are low for short periods and tend to be high for longer periods (> 1s) in almost all transect, excepting the southernmost sector. The high phase values are associated to conductive structures at lower crust and upper mantle depths. Northwards a phase disagreement between TE and TM modes can be noted: for all period range, with TE mode exhibiting anomalous negative values, while TM mode shows anomalously high values (above 90°).

The tipper magnitude seems to indicate a highly tri-dimensional region associated with the resistive central block observed in both TE and TM mode pseudosections.

## Conclusions

The results currently suggest the presence of a resistive block at the central traverse sector, consistent with the existence of a cratonic fragment deep rooted at that place. Extensive conductors are shown at the south and north limits of the central resistive block, possibly extending towards its base, suggesting previous lithospheric hydration and currently the presence of chemically enriched mineral phases. Anomalous phases either exceeding 90° or achieving negative values, as well as the disagreement between tipper and apparent resistivity information, could indicate the presence of not only galvanic and inductive distortion but also anisotropy. Tridimensional inversion is indicated for this profile and results must benefit from appropriate complementary forward modelling as well as other available geophysical and geological information.

## References

**BIBBY, H.M., CALDWELL, T. G., & BROWN, C.** (2005). *Determinable and non-determinable parameters of galvanic distortion in magnetotellurics.* Geophys. J. Int., 163: 915–930.

**CALDWELL, T.G., BIBBY, H.M., AND BROWN, C.** (2004). *The magnetotelluric phase tensor.* Geophysical Journal International. 158: 457-469.

**EGBERT, G.D. AND D.W. LIVELYBROOKS.** (1996). *Single station magnetotelluric impedance estimation: coherence weighting and the regression M-estimate.* Geophysics. (61): 964-970.

**EGBERT, G.D., AND BOOKER, J.R.** (1986). *Robust estimation of geomagnetic transfer functions.* Geophys. J. R. astr. Soc., 87, 173-194.

**EGBERT, G.D.; EISEL, M**. (1998). *Programs for Robust Single station and Remote reference analysis of Magnetotelluric data: Unix (and PC) version.* Disponível em: www.cg.nrcan.gc.ca/mtnet.

**HEINSON, G., DIREEN, N. AND GILL, R.M.,** (2006). *Magnetotelluric evidence for a deep-crustal mineralizing system beneath the Olympic Dam iron oxide copper-gold deposit, southern Australia.* Geology, 34, 573–576.

**KRIEGER, L., AND PEACOCK, J.R**. (2014). *MTpy: A Python toolbox for magnetotellurics*. Computers & Geosciences, 72, 167–175.

**MAIER, R., HEINSON G., THIEL S., SELWAY K., GILL R., SCROGGS M.** (2007). *A 3D lithospheric electrical resistivity model of the Gawler Craton, Southern Australia.* Transactions of the Institutions of Mining and Metallurgy, Section B: Applied Earth Science. 116(1): 13-21.

**MARTÍ, A., QUERALT, P., & LEDO, J.** (2009). *WALDIM: A code for the dimensionality analysis of magnetotelluric data using the rotational invariants of the magnetotelluric tensor*. Computers & Geosciences, 35: 2295–2303.

**MARTI, A., QUERALT, P., JONES, A.G., & LEDO, J.,** 2005. *Improving Bahr's invariant parameters using the WAL approach.* Geophysical Journal International, 163: 38–41.

**PADILHA, A. L.** (1999), *Behaviour of magnetotelluric source fields within the equatorial zone.* Earth, Planets, and Space, 51, 1119–1125.

**PADILHA, A. L., VITORELLO, I., RIJO, L.** (1997), *Effects of the equatorial electrojet on magnetotelluric surveys: Field results from northwest Brazil*. Geophysical Research Letters, 24(1), 89–92.

**SCANDOLARA, J.E.; CORREA, R.T.; FUCK, R.A.; SOUZA, V.S.; RODRIGUES, J.B.; RIBEIRO, P.S.E.; FRASCA, A.A.S.; SABOIA, A.M.; LACERDA FILHO, J.V.** (2017). *Paleo-Mesoproterozoic arc-accretion along the southwestern margin of the Amazonian craton: The Juruena accretionary orogen and possible implications for Columbia supercontinent.* Journal of South American Earth Sciences. 73: 223-247.

**SPRATT, J. E., T. SKULSKI, J. A. CRAVEN, A. G. JONES, D. B. SNYDER, AND D. KIYAN** (2014). *Magnetotelluric investigations of the lithosphere beneath the central Rae craton, mainland Nunavut, Canada.* J. Geophys. Res. Solid Earth, 119: 415–439.

**TASSINARI, C.C.G. & MACAMBIRA, M.J.B.** (2004). *A Evolução Tectônica Do Cráton Amazônico*. In: Mantesso-Neto, V.; Bartorelli, A.; Carneiro, C.D.R.; Brito Neves, B.B. (eds.). Geologia do Continente Sul-Americano: Evolução da Obra de Fernando Flávio Marques de Almeida. São Paulo. 471-485.

**WEAVER, J. T.; AGARWAL, A. K.; LILLEY, F.E.M**. (2000). *Characterization of themagnetotelluric tensor in terms of its invariants.* Geophys. J. Int. 141: 321-336.

**WEAVER, J. T., AGARWAL, A. K., & LILLEY, F. E. M**. (2006). *The relationship between the magnetotelluric tensor invariants and the phase tensor of Caldwell, Bibby and Brown*. Explor. Geophys. 37: 261 – 267

## Acknowledgments

The research project was supported by the Geophysics Graduate Study Program of Observatório Nacional (ON) and by the Geological Survey of Brazil (CPRM). C.M. Fernandes would like to thank CAPES for the awarding of her master scholarship. The authors would like to thank Dr Marcelo Banik for making available some code implementations employed on MT data processing.

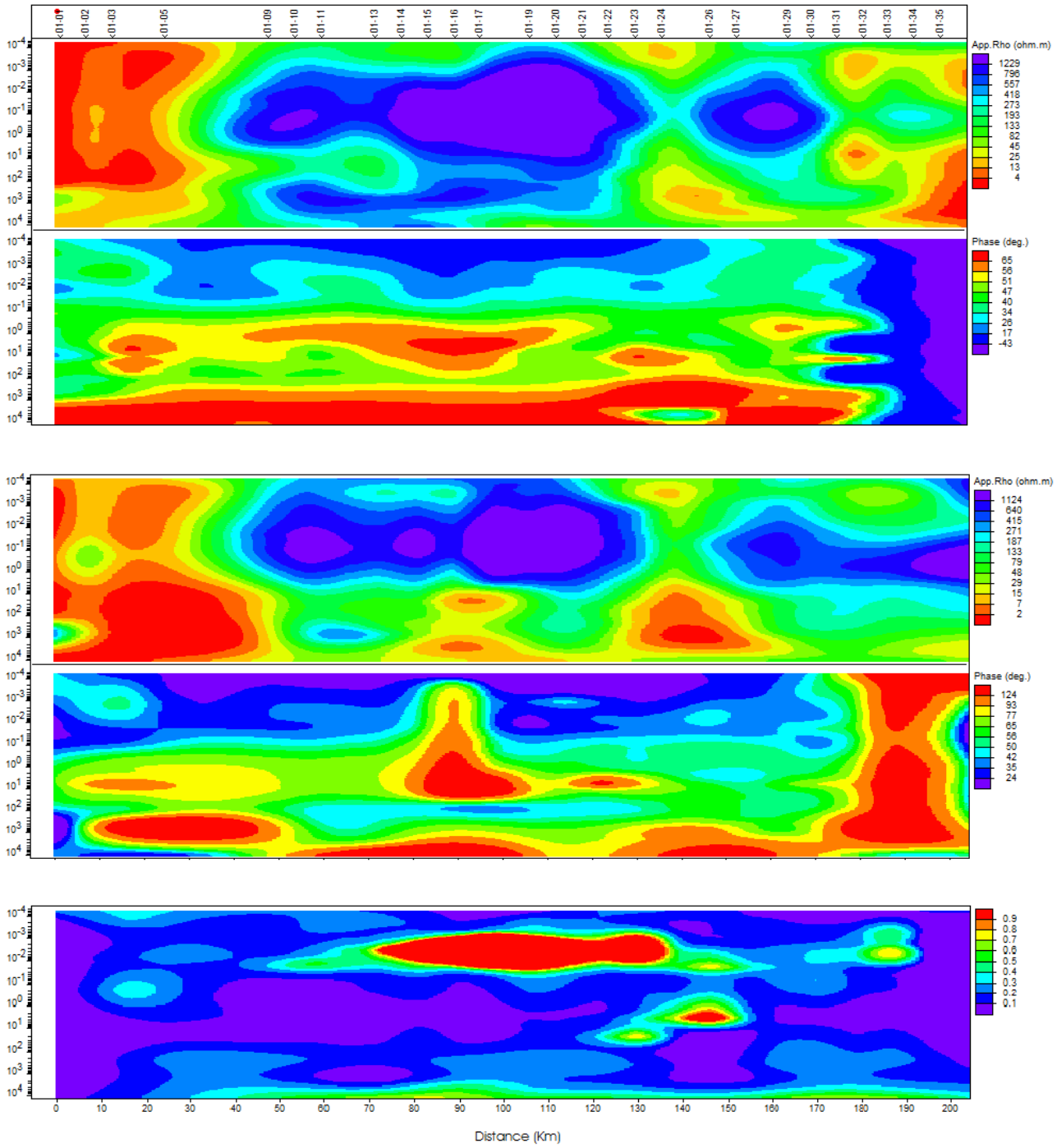


***Figure 6:*** *Pseudosections: apparent resistivity and phase versus period for TE mode; apparent resistivity and phase versus period for TM mode; and tipper magnitude versus period, respectively.*